

1 **Generating closed bacterial genomes from long-read nanopore sequencing of**  
2 **microbiomes**

3 Eli L. Moss<sup>1</sup>, Ami S. Bhatt<sup>1,\*\*</sup>

4 <sup>2</sup>Department of Medicine (Hematology, Blood and Marrow Transplantation) and Department of  
5 Genetics, Stanford University, Stanford, California, USA.

6 <sup>\*\*</sup> To whom correspondence should be addressed: [asbhatt@stanford.edu](mailto:asbhatt@stanford.edu)

## 7 **Abstract**

8           We present the first method for efficient recovery of complete, closed genomes directly  
9 from microbiomes using nanopore long-read sequencing and assembly. We apply our approach  
10 to three healthy human gut communities and compare results to short read and read cloud  
11 approaches. We obtain nine finished genomes including the first reported closed genome of  
12 *Prevotella copri*, an organism with highly repetitive genome structure prevalent in non-western  
13 human gut microbiomes.

## 14 **Main Text**

15 *De novo* reconstruction of complete microbial genomes from metagenomes has been a  
16 longstanding goal of microbiome research. Although current reference-based methods are able  
17 to detect known organisms and genes in metagenomes, only *de novo* approaches are able to  
18 characterize novel genome sequences, or accurately place mobile or transferred elements in  
19 new genomic contexts. The tremendous diversity and plasticity of bacterial genomes, as well as  
20 the difficulty of bacterial isolation and culture, demand effective culture-free methods for  
21 producing genomes directly from metagenomes.

22 Current metagenomic sequencing and assembly methods do not typically yield finished  
23 bacterial genomes, although previous efforts have achieved single closed genomes in simple  
24 communities<sup>1</sup>, or multiple genomes with skilled manual assembly and scaffolding<sup>2</sup>.  
25 Consequently, genome drafts are formed by grouping (i.e. binning) similar contigs within  
26 fragmentary assemblies<sup>3,4</sup>. This is an imperfect process, often compromising the purity or the  
27 completeness of the genome reconstruction. As assembly contiguity increases, the sensitivity  
28 and specificity of genome binning are improved as fewer, larger contigs need to be grouped to  
29 form each genome. Indeed, at the point when genomes are assembled in single contigs, binning  
30 becomes unnecessary. Nanopore long read assembly has yielded complete genomes in  
31 cultured bacterial isolates<sup>5-8</sup>, suggesting potential for effective assembly in more complex  
32 microbial communities. However, the performance of nanopore and other long read approaches  
33 in metagenomic sequencing and assembly has been limited by the lack of effective and efficient  
34 methods to maximize molecular weight, mass yield and purity of DNA extracted from these  
35 samples.

36 We present a workflow consisting of stool DNA extraction, nanopore sequencing,  
37 assembly and post-processing steps capable of producing multiple complete, circular bacterial  
38 genomes directly from metagenomes. Our extraction approach produces microgram quantities  
39 of pure, high molecular weight (HMW) DNA suitable for long read sequencing from as little as

40 300 milligrams (mg) of stool. Our computational workflow, consisting of assembly and post-  
41 processing, does not involve manual intervention in assembly, scaffolding, bacterial isolation, or  
42 existing reference coverage of the target metagenome. Thus, this workflow is the first to provide  
43 a rapid, simple, cost-effective, automated approach to close high numbers of bacterial genomes  
44 directly from metagenomic samples.

45 Short read and read cloud data and assemblies for samples P1 and P2-A were used  
46 without modification as previously described<sup>9</sup>. The standard approach used to extract DNA for  
47 these libraries produced fragmented DNA which incurred a severe loss with size selection,  
48 necessitating approximately 300 mg input stool to assure the 1 nanogram (ng) final HMW DNA  
49 mass required for read cloud library preparation. Current long read library prep protocols require  
50 1000 ng of HMW input DNA, well beyond the practical capability of existing stool DNA extraction  
51 techniques. In order to maximize the throughput and read length of nanopore sequencing, a  
52 new approach yielding DNA in dramatically higher quantity and molecular weight was needed.

53 We developed a method for HMW extraction capable of yielding 1000-fold more DNA  
54 over 5 kb than a conventional bead-beating approach (Supplementary Figure 1, see Methods).  
55 We applied this method to two samples (P1 and P2-A) as well as a third sample (P2-B),  
56 collected 15 months later from the second individual. HMW DNA extraction yielded at least 1 µg  
57 HMW DNA per 300 mg input stool mass for all samples (Supplementary Table 1). Nanodrop  
58 measurement produced  $A_{260/280}$  ratios over 1.86 and  $A_{260/230}$  ratios over 2.23 for all samples,  
59 indicating absence of contaminants such as proteins, solvents and salts.

60 We obtained a total of 12.7 giga-base pairs (Gbp), 6.1 Gbp, and 7.6 Gbp of long read  
61 data for samples P1, P2-A, and P2-B, respectively (Supplementary Figure 2, Supplementary  
62 Table 2) with N50 values of 4.7 kbp, 3 kbp and 3 kbp. The taxonomic composition of reads  
63 obtained through our approach was compared to that obtained by standard mechanical lysis  
64 and short read sequencing methods (see Methods). Although precise rank order relative  
65 abundances varied, we noted higher Shannon diversity from the present approach (P2: 2.0 vs.

66 1.14; P1: 2.0 vs. 1.8). We also detected all genera represented by more than 200 short reads  
67 from the traditional short read sequencing in the long read data.

68 Our assembly and post-processing workflow yielded whole-assembly N50 values of 453  
69 kbp, 571 kbp and 564 kbp for the three samples P1, P2-A and P2-B. In comparison, the short  
70 read approach did not exceed assembly N50 of 34 kbp across samples P1 and P2-A, in spite of  
71 3- to 6-fold more read data (37-38 Gbp). Our approach also surpassed the read cloud N50  
72 values of 116 kbp and 12 kbp. However, read cloud and short read assemblies were between  
73 1.5- and 2.1-fold larger than corresponding long read assemblies, likely due to the much greater  
74 volume of raw data available from these datasets (Supplementary Table 3).

75 Contigs from each approach were binned to form draft genomes, which were evaluated  
76 and assigned 'High Quality', 'Complete' and 'Incomplete' labels as described<sup>9</sup>. Briefly, drafts at  
77 least 90% complete and with at most 5% contamination are termed 'Complete', and drafts also  
78 containing at least one each of the 5S, 16S and 23S rRNA loci, as well as at least 18 tRNA loci,  
79 are labeled 'High Quality'. All others are 'Incomplete'. While read cloud and short read methods  
80 produced more complete bins and a comparable number of high quality bins compared to the  
81 long read approach, the long read approach produced bins with much higher contiguity (Figure  
82 1). The present approach yielded nine high quality genomes with N50 over 2 Mbp, whereas the  
83 read cloud approach yielded only one. Short read bins never exceeded 550 kbp. Finally, the  
84 present approach yields a comparable quantity of high quality genomes at far higher contiguity  
85 with lower capital equipment requirement, sequencing cost and turnaround time (Supplementary  
86 Table 4).

87 Nanopore long read assembly yielded nine complete, circularizeable bacterial genomes  
88 across the three sequenced samples, and a maximum of four from a single sample (P1),  
89 compared to zero from the short read, read cloud, and synthetic long read approaches  
90 previously applied to these samples<sup>9</sup>. Assembled genomes are up to 5Mbp in length, and in  
91 several cases (*Prevotella copri*, *Subdoligranulum variabile*, *Phascolarctobacterium faecium*, and

92 *Bacteroides uniformis*) represent the first closed genomes for their species. Closed genomes  
93 ranged in coverage depth between 75 (*Oscillibacter* sp.) and 785 (*P. copri*). Closed genomes  
94 were largely structurally concordant and similar in sequence to existing published genome  
95 sequences (Supplementary Figure 3, Supplementary Table 5), although in some cases we do  
96 note extensive strain divergence; for example, our closed *Dialister invisus* genome exhibits  
97 multiple large-scale inversions relative to the available reference (see below).

98 Completed bacterial genomes included two for *Prevotella copri* in samples P2-A and P2-  
99 B. This organism lacks a closed reference, in spite of extensive efforts to assemble *P. copri* and  
100 other members of the genus *Prevotella*<sup>10</sup>. Our previous efforts using read clouds, short reads  
101 and synthetic long reads to assemble these communities also had limited success with this  
102 organism, never exceeding a genome N50 of 130 kbp, in spite of coverage depth in excess of  
103 4,800x<sup>9</sup>. The two *P. copri* genomes obtained from samples separated by 15 months display high  
104 concordance, with 99.94% of bases aligned and 99.89% nucleotide identity, suggesting nearly  
105 identical strain composition in the two time points.

106 The difficulty of assembling the *P. copri* genome stems from its high degree of sequence  
107 repetition. A direct assembly of highly abundant *k*-mers ( $k=101$ , occurring more than 5 times)  
108 found in our complete genome assembly yielded two insertion sequences (ISs) (see Methods),  
109 one 1.1 kbp IS66 family sequence and one 1.6 kbp IS1380 family sequence. These were found  
110 to be assembled in a total of 29 genomic loci between the two timepoints, but IS instances  
111 absent from the consensus assembly were detected directly in long reads at an additional 45  
112 loci (see Methods). These insertion sites, whether fixed in the strain population or varying  
113 between strains, co-locate with breaks in short read and read cloud assemblies, illustrating their  
114 impact on these types of assembly (Figure 2).

115 Other complete genomes include *Phascolarctobacterium faecium* assembled in samples  
116 P2-A and P2-B at relative abundances of 4% and 1.41%, respectively. These assemblies are  
117 the first complete genomes for this species, and display high structural and nucleotide

118 concordance with the closest available reference (Supplementary Figure 3; 98.9% identity,  
119 88.5% sequence alignment) and with each other (99.81% identity, 99.97% sequence  
120 alignment). Sample P2-A also yielded the first circular genome for *Dialister invisus*, present in  
121 that sample at 1.03% relative abundance. We find similar structural divergence compared to the  
122 available reference (Supplementary Figure 3), and concordance with the read cloud draft, which  
123 contained identical large-scale structural inversions (99.90% identity, 99.97% sequence  
124 alignment) (Figure 2, Supplementary Table 5). Although the *Dialister invisus* assembled in  
125 sample P2-B was assessed complete, it was not found to be circularizable.

126 In sample P1, we obtained circular genomes for *Bacteroides uniformis* (6% abundance  
127 in long reads), *Alistipes finegoldii* (2% abundance), *Oscillibacter sp.* (0.14% abundance), and  
128 *Subdoligranulum variabile* (0.37% abundance). Of these, we were able to obtain structurally  
129 concordant reference sequences for all but *Subdoligranulum*, for which we could not locate a  
130 reference with more than 19% aligned bases, suggesting the possibility of a novel strain. Seven  
131 16S rRNA loci were assembled in this genome, all bearing 98% sequence identity to the closest  
132 match from *Subdoligranulum variabile* strain BI114, for which no genome reference is available  
133 for comparison. Identity with read cloud assemblies in all cases was over 99.7%, with over  
134 98.3% of bases aligning to the assembled draft (Supplementary Table 5). For all closed  
135 genomes, read cloud and short read assembly yielded more fragmentary assemblies, which  
136 were only partially recovered by binning (Figure 2).

137 Our approach relies on consensus refinement based on short read data to correct  
138 homopolymer errors intrinsic to the current nanopore sequencing technology. Although long  
139 read-based consensus refinement is possible and partially effective, we find that it cannot fully  
140 replace short read correction (Supplementary Figure 4). We found that uncorrected long read  
141 assembly demonstrated a 3% error rate with 3-mer homopolymers, assembled too short by an  
142 average of 0.5 nucleotides. This worsens to a 65% error rate on 6-mer homopolymers, which  
143 were assembled too short by an average of 1.3 nucleotides. On average, 63 homopolymers of

144 length 3 or greater were found per kilobase of assembled sequence, of which 4.5 (7.1%) were  
145 found to require correction with short reads. CheckM, a tool which annotates genome  
146 completeness based on single copy core gene detection, demonstrates a low detection rate on  
147 uncorrected assemblies, consequently under-reporting genome completeness even on  
148 circularizeable whole-genome contigs. For instance, the genome annotated *Oscillibacter sp.* in  
149 sample P1 is annotated 38% complete in the uncorrected assembly. This rises to 68% complete  
150 after correction with long reads. With short read correction, the genome receives a 96%  
151 completeness annotation, compared to 98% for the sole available closed genome reference  
152 sequence (strain PEA192). The present workflow for sequencing and assembly can operate  
153 solely with long reads and will yield structurally correct and complete genomes, although with  
154 reduced nucleotide accuracy. Future advances in nanopore sequencing technology that  
155 decrease the homopolymer-repeat related errors will likely lessen or remove the requirement for  
156 supplemental short read sequencing to achieve genomes with high nucleotide fidelity.

157         Although the present approach has achieved effective assembly of bacterial genomes  
158 from metagenomes, we anticipate that future advances in metagenomic DNA extraction  
159 methods and nanopore long read assembly will improve read length and reduce the read  
160 coverage required to close genomes. In addition, epigenetic modification detection will add to  
161 future metagenomic studies by revealing phage and bacterial sequence methylation patterns,  
162 methylation-based contig binning approaches, and epigenetic regulation of bacterial DNA-  
163 protein interactions.

164         In conclusion, our approach assembles the first complete genome of *Prevotella copri*, an  
165 organism with high prevalence in non-western guts and with emerging, potentially strain-specific  
166 links to human health and disease<sup>11,12</sup>. The high copy number of IS66 and IS1380 family  
167 insertion sequences in this genome limit the effectiveness of short read approaches, despite  
168 receiving over 4,800x coverage in an earlier metagenomic sequencing study<sup>9</sup> and extensive  
169 isolate sequencing in a separate effort<sup>10</sup>. IS1380 has been previously reported to carry an



170 outward-facing promoter capable of upregulating adjacent gene sequences, and has been  
171 found to impact antibiotic resistance gene regulation and resistance phenotype<sup>13</sup>. We anticipate  
172 that this approach will help illuminate the role of repetitive classes of genomic elements with  
173 important effects on cellular and clinical phenotypes, and facilitate efforts to broaden human  
174 microbiome research to global populations where *Prevotella* are highly prevalent<sup>14</sup>. Closing  
175 these and other genomes will allow investigation into the complete functional repertoire and  
176 potential phenotypes of individual microbes, even when these organisms are difficult to culture  
177 or are found in mixed communities, facilitating future research in important human microbiomes  
178 and poorly characterized microbial communities such as soil and marine sediment.

179 **Bibliography**

- 180 1. Leonard, M.T. et al. *Front. Microbiol.* **5**, 361 (2014).
- 181 2. Anantharaman, K. et al. *Nat. Commun.* **7**, 13219 (2016).
- 182 3. Bowers, R.M. et al. *Nat. Biotechnol.* **35**, 725–731 (2017).
- 183 4. Kang, D.D., Froula, J., Egan, R. & Wang, Z. *PeerJ* **3**, e1165 (2015).
- 184 5. Koren, S. & Phillippy, A.M. *Curr. Opin. Microbiol.* **23**, 110–120 (2015).
- 185 6. Risse, J. et al. *Gigascience* **4**, 60 (2015).
- 186 7. Turner, D.J., Dai, X., Mayes, S. & Juul, S. *bioRxiv* 026930 (2015).
- 187 8. Loman, N.J., Quick, J. & Simpson, J.T. *Nat. Methods* **12**, 733–735 (2015).
- 188 9. Bishara, A. et al. *Nat. Biotechnol.* (2018).doi:10.1038/nbt.4266
- 189 10. Gupta, V.K., Chaudhari, N.M., Iskepalli, S. & Dutta, C. *BMC Genomics* **16**, 153 (2015).
- 190 11. Scher, J.U. et al. *eLife Sciences* **2**, e01202 (2013).
- 191 12. Pianta, A. et al. *Arthritis & Rheumatology* **69**, 964–975 (2017).
- 192 13. Kato, N., Yamazoe, K., Han, C.-G. & Ohtsubo, E. *Antimicrob. Agents Chemother.* **47**, 979–
- 193 985 (2003).
- 194 14. Schnorr, S.L. et al. *Nat. Commun.* **5**, 3654 (2014).
- 195 15. Mukhopadhyay, T. & Roth, J.A. *Nucleic Acids Res.* **21**, 781–782 (1993).
- 196 16. Not provided, R. & Schwessinger, B.doi:10.17504/protocols.io.n7hdhj6
- 197 17. Koren, S. et al. *Genome Res.* (2017).doi:10.1101/gr.215087.116
- 198 18. Chakraborty, M., Baldwin-Brown, J.G., Long, A.D. & Emerson, J.J. *Nucleic Acids Res.* **44**,
- 199 e147 (2016).
- 200 19. Hunt, M. et al. *Genome Biol.* **16**, 294 (2015).
- 201 20. at <<https://nanoporetech.github.io/medaka/index.html>>
- 202 21. Walker, B.J. et al. *PLoS One* **9**, e112963 (2014).
- 203 22. Danecek, P., McCarthy, S., Li, H. & Others (2015).

- 204 23. Delcher, A.L., Salzberg, S.L. & Phillippy, A.M. *Curr. Protoc. Bioinformatics* **00**, 10.3.1–  
205 10.3.18 (2003).
- 206 24. Parks, D.H., Imelfort, M., Skennerton, C.T., Hugenholtz, P. & Tyson, G.W. *Genome Res.*  
207 **25**, 1043–1055 (2015).
- 208 25. Wood, D. & Salzberg, S. *Genome Biol.* **15**, R46 (2014).
- 209 26. Dixon, P. *J. Veg. Sci.* **14**, 927–930 (2003).
- 210 27. Wickham, H. (Springer Science & Business Media: 2009).
- 211 28. Hahne, F. & Ivanek, R. *Methods Mol. Biol.* **1418**, 335–351 (2016).
- 212 29. Højsgaard, S., Højsgaard, M.S. & Hmisc, D. *The Newsletter of the R Project* **6**, 1 (2006).
- 213 30. Wickham, H. *R package version 1*, (2012).
- 214 31. Köster, J. & Rahmann, S. *OASlcs-OpenAccess Series in Informatics* **26**, (2012).
- 215 32. Marçais, G. & Kingsford, C. *Bioinformatics* **27**, 764–770 (2011).
- 216 33. Bankevich, A. et al. *J. Comput. Biol.* **19**, 455–477 (2012-5).
- 217 34. Li, H. *Bioinformatics* **34**, 3094–3100 (2018).

218 **Methods**

219 DNA extraction

220 Short read and read cloud libraries were prepared as previously described<sup>9</sup>. Previously,  
221 DNA was extracted from samples P1 and P2-A with a commercial extraction kit using bead-  
222 beating lysis.

223 For high molecular weight (HMW) extraction, approximately 0.7g frozen stool was  
224 aliquoted into 2mL eppendorf tubes (Eppendorf, Hamburg, Germany) with a 4mm biopsy punch  
225 (Integra Miltex, Plainsboro, NJ) and suspended in 500 $\mu$ L PBS (Fisher Scientific, Waltham, MA)  
226 with brief gentle vortexing. 5 $\mu$ L of lytic enzyme solution (Qiagen, Hilden, Germany) was added  
227 and the samples were mixed by gentle inversion six times, then incubated for one hour at 37°C.  
228 12 $\mu$ L 20% (w/v) SDS (Fisher Scientific, Waltham, MA) was added with approximately 100 $\mu$ L  
229 vacuum grease (Dow-Corning, Midland, MI) functioning as phase lock gel<sup>15</sup>. 500 $\mu$ L phenol  
230 chloroform isoamyl alcohol at pH 8 (Fisher Scientific, Waltham, MA) was added, and samples  
231 were gently vortexed for five seconds, then centrifuged at 10,000g for five minutes with Legend  
232 Micro 21 microcentrifuge (Fisher Scientific, Waltham, MA). The aqueous phase was then  
233 decanted into a new 2mL tube.

234 Next, DNA was precipitated with 90 $\mu$ L 3M sodium acetate (Fisher Scientific) and 500 $\mu$ L  
235 isopropanol (Fisher Scientific) for ten minutes at room temperature. After inverting three times  
236 slowly, samples were incubated at room temperature for 10 minutes, then centrifuged 10  
237 minutes at 10,000g. The supernatant was removed and the pellet was washed two times with  
238 freshly prepared 80% (v/v) ethanol (Fisher Scientific). The pellet was then air dried with heating  
239 for ten minutes at 37°C or until the pellet was matte in appearance, and then resuspended in  
240 100 $\mu$ L nuclease-free water (Ambion, Thermo Fisher Scientific, Waltham, MA). 1mL Qiagen  
241 buffer G2, 4 $\mu$ L Qiagen RNase A at 100mg/mL, and 25 $\mu$ L Qiagen Proteinase K were added, the  
242 samples were then gently inverted three times, and then were incubated 90 minutes at 56°C.  
243 After the first 30 minutes, pellets were dislodged by a single gentle inversion.

244 One Qiagen Genomic-tip 20/G column per sample was equilibrated with 1mL Qiagen  
245 buffer QBT and allowed to empty by gravity flow. Samples were gently inverted twice, applied  
246 to columns and allowed to flow through. Three stool extractions were combined per column.  
247 Columns were then washed with 3mL Qiagen buffer QC, then DNA was eluted with 1mL Qiagen  
248 buffer QF prewarmed to 56°C. Eluted DNA was then precipitated by addition of 700µL  
249 isopropanol followed by inversion and centrifugation for 15 minutes at 10,000g. The  
250 supernatant was carefully removed by pipette, and pellets were washed with 1mL 80% (v/v)  
251 ethanol. Residual ethanol was removed by air drying ten minutes at 37°C. This was followed by  
252 resuspension of the pellet in 100µL water overnight at 4°C without agitation or any kind.

253 DNA was then size selected with a modified SPRI bead protocol as described <sup>16</sup>, with  
254 minor modifications: beads were added at 0.9x, and eluted DNA was resuspended in 50µL  
255 water. The concentration, purity and fragment size distribution of extracted DNA was then  
256 quantified with the Qubit fluorometer (Thermo Fisher Scientific, Waltham, MA), Nanodrop  
257 (Thermo Fisher Scientific), and Tapestation 2200 (Agilent Technologies, Santa Clara, CA),  
258 respectively (Supplementary Table 1).

259

## 260 Sequencing

261 Extracted DNA samples were prepared for long read sequencing with the Oxford  
262 Nanopore Technologies (ONT, Oxford, UK) Ligation library preparation kit according to the  
263 manufacturer's standard protocol. Libraries were sequenced with the ONT MinION sequencer  
264 using rev C R9.4 flow cells, allocating one flowcell per sample. The sequencer was controlled  
265 with the MinKNOW v2.2.12 software running on a MacBook Pro (model A1502, Apple,  
266 Cupertino, CA), with data stored to a Vectotech 2Tb SSD hard drive. Sequencing runs were  
267 scheduled for 48 hours, and allowed to run until fewer than 10 pores remained functional. After  
268 sequencing, data were uploaded to the Stanford Center for Genomics computational cluster for

269 analysis (see below). Short read libraries were prepared and sequenced as described  
270 previously<sup>9</sup>.

271

## 272 Sequence assembly and analysis

273 Raw data were basecalled with Albacore v2.3.1, and assembled in two separate runs  
274 with Canu v1.7.1 with the -nanopore preset parameter<sup>17</sup>. The two runs differed by the estimated  
275 genomeSize parameter, provided as either 50m or 100m. The two separate assemblies were  
276 then merged with quickmerge v0.40<sup>18</sup>, circularized with Circlator v1.5.5<sup>19</sup> and Encircle (present  
277 study, see below), and then polished with either Medaka<sup>20</sup> or a parallelized version of Pilon  
278 v1.22<sup>21</sup> (present study) for long read or short read consensus refinement, respectively. In order  
279 to parallelize Pilon, reference sequences were divided into 100kb segments, short reads  
280 aligning to each segment were downsampled to at most 40x coverage depth, and Pilon was  
281 used to detect errors within the reference and read subset. These errors were then aggregated  
282 across all subset runs and used to generate a refined consensus with bcftools<sup>22</sup>. Errors found in  
283 homopolymers were identified with an in-house script, homopolymer\_error\_analyzer.  
284 Sequences are binned and annotated as previously described<sup>9</sup>.

285 There is presently no straightforward, comprehensive method for determining circularity  
286 in metagenome-assembled genomes. A minority of the circular genomes we obtained (*D.*  
287 *invisus* in P2-A, *P. copri* and *Phascolarctobacterium* in P2-B) were circularized by an existing  
288 genome circularization tool. In several cases, assembled genome contigs extended beyond the  
289 wrap-around point of the circular chromosome, resulting in what we term over-circularization  
290 (supp fig 5). Over-circularized contigs contain redundant sequences at their termini which  
291 spuriously increase apparent contamination when assessed by CheckM. In order to trim over-  
292 circularized contig ends in order to obtain a nonredundant, circular genome, we developed  
293 Encircle, a utility which performs contig self-alignment with Mummer<sup>23</sup> and determines when  
294 over-circularization has taken place, then outputs precise trim coordinates to circularize the

295 genome. The genomes of *P. copri*, *Phascolarctobacterium sp.*, and *Dialister invisus* in sample  
296 P2-A, as well as *Oscillibacter sp.* and *Subdoligranulum* (supp figure 5) in sample P1, were over-  
297 circularized and required trimming. In addition, the genomes of *Bacteroides uniformis* and  
298 *Alistipes finegoldii* were determined to be circular by concatenating the first and last 20kbp of  
299 the assembled genome, mapping long reads to the junction, and inspecting alignments for  
300 reads spanning the gap; *B. uniformis* was found to be slightly overcircularized by 10kbp (below  
301 the limit of detection of Encircle), and *A. finegoldii* was found to be perfectly circularizeable.

302 Binning was performed and evaluated as previously described<sup>9</sup>. Due to the complete  
303 genomes present in our assemblies, binning became unnecessary for some organisms, and  
304 instead led to several cases of genomic contamination as assessed with CheckM. In cases  
305 where >5% contamination occurred in a bin with one genome-scale contig and several much  
306 smaller (<100kbp) sequences, the smaller sequences were removed and the largest sequence  
307 was re-evaluated with CheckM<sup>24</sup>, in two cases yielding complete and uncontaminated genomes.

308 Long and short reads were taxonomically classified with Kraken<sup>25</sup>, and Shannon  
309 diversity was calculated with vegan<sup>26</sup>. Figures were generated with ggplot2<sup>27</sup>, gviz<sup>28</sup>, doBy<sup>29</sup> and  
310 reshape2<sup>30</sup>. All workflows were implemented with Snakemake<sup>31</sup>.

311

### 312 Insertion sequence strain diversity

313 K-mers represented more than 6 times in the *Prevotella copri* assemblies were identified  
314 with Jellyfish<sup>32</sup>. These were assembled with SPAdes<sup>33</sup> to obtain two full-length insertion  
315 sequences. These sequences were located in the genome assemblies by alignment with  
316 minimap2<sup>34</sup>. In order to locate additional unassembled insertion sequences present in strains of  
317 *P. copri*, reads containing insertion sequences were identified by alignment with minimap2, then  
318 200 bases immediately upstream of the insertion sequence were taken from each read and  
319 aligned to the genome assembly.

320 In order to quantify the relative abundance of *P. copri* strains carrying each IS instance,  
321 long reads were first aligned to the assembled IS sequences. Long reads containing IS  
322 sequences were isolated, and flanking sequences 200bp upstream of the IS were extracted and  
323 realigned to the genome assembly. IS-flanking sequence depth was compared to local overall  
324 coverage depth to obtain the relative abundance of strains carrying a given IS. Only 18 insertion  
325 sites carried fixed ISs and a further 56 sites showed a mixture of strains with and without an IS  
326 (Figure 2).

327

#### 328 Data availability

329 All sequence data, whole metagenome assemblies and individual completed genomes  
330 can be found at NCBI BioProject under accession PRJNA508395.

331

#### 332 Code availability

333 All workflows and associated environments and tools can be found at  
334 [https://github.com/elimoss/metagenomics\\_workflows/](https://github.com/elimoss/metagenomics_workflows/).



## 335 **Acknowledgements**

336           The authors would like to acknowledge Gavin Sherlock and the members of the Bhatt  
337 lab for helpful advice and assistance. E.L.M. was supported by National Science Foundation  
338 Graduate Research Fellowship DGE-114747. This work was supported by the Damon Runyon  
339 Clinical investigator award to ASB. Computational work was supported by NIH S10 Shared  
340 Instrumentation Grant 1S10OD02014101.

341

## 342 **Competing financial interests**

343 The authors declare no competing financial interests.

344

## 345 **Figure Legends**

### 346 Figure 1

347 Taxonomic read composition and per-organism assembly contiguity for healthy gut assemblies,  
348 overall genome draft counts in two healthy human gut microbiomes (samples P1, P2-A).  
349 Nanopore sequencing and assembly (blue) demonstrates better assembly contiguity than read  
350 cloud (gold) and short read (green) approaches, but produced a smaller overall assembly with  
351 fewer complete drafts at the overall sequence coverage obtained. (a) Relative genus-level  
352 abundances are shown for a conventional workflow consisting of bead-beating extraction and  
353 short read sequencing, as well as the present workflow consisting of high molecular weight DNA  
354 extraction and long read sequencing. (b) For all organisms achieving assembly N50 of at least  
355 500 kbp by any approach, genome draft quality and contiguity are shown for long reads, read  
356 clouds and short reads. Shapes indicate draft quality. Circularized genomes are indicated by  
357 green circles. (c) Complete genome bins with a minimum N50. (d) Complete genome bins below  
358 a given read coverage depth. Genome bins with lower read coverage originate from less  
359 abundant organisms. (e) Complete genome bins with N50 of > 2 Mbp below a given read  
360 coverage depth. (f) High quality genome bins with a minimum N50. (g) High quality genome bins

361 below a given depth of read coverage. (h) High quality genome bins with an N50 exceeding 2  
362 Mbp below a given read coverage depth.

363

364 Figure 2

365 Genome assemblies, repeat structure and relative insertion sequence strain abundances of  
366 *Prevotella copri* and genome assembly comparisons for other closed genome assemblies. The  
367 *Prevotella copri* genome is difficult to assemble beyond insertion sequence sites due to their  
368 repetitiveness. For this reason, short read (green) and read cloud (gold) assemblies are highly  
369 fragmentary despite very high coverage (>4000x coverage depth). Long reads achieve a closed  
370 genome in spite of much lower coverage (318x) (blue). Relative abundances of strains carrying  
371 each insertion sequence instance are shown for 0-month and 15-month timepoints (first and  
372 second tracks), as well as log-fold change at each site between the two timepoints (third track).  
373 b) Finished genomes assembled by the present workflow (blue) are shown with corresponding  
374 bins obtained from read cloud (gold) and short read (green) approaches. Read cloud and short  
375 read approaches yield more fragmentary approaches, with large genomic regions missing due  
376 to incomplete binning.

## 377 **Supplementary Figure Legends**

### 378 Supplementary Figure 1

379 Overview of the molecular and informatic workflow steps. a) Extraction consists of  
380 enzymatic degradation of bacterial cell walls followed by an initial DNA extraction in phenol-  
381 chloroform. This is followed by a proteinase K and RNase A digestion at high temperature and  
382 purification with a gravity column. Finally, small fragments are removed by modified SPRI bead  
383 size selection. b) After sequencing and basecalling, read sequences are assembled twice with  
384 varying genomeSize parameter values. These two assemblies are merged, then circular  
385 sequences are identified and trimmed. The consensus sequence is refined by either short-read  
386 or long-read polishing.

387

### 388 Supplementary Figure 2

389 Histogram of total bases versus read length for the three samples sequenced with the  
390 current approach. Read lengths vary between <1kbp to >100kbp, with N50 values between  
391 5kbp and 10kbp.

392

### 393 Supplementary Figure 3

394 Reference alignment dotplots for closed genomes obtained by nanopore long read  
395 sequencing and assembly. Although assemblies share broad structural similarity to available  
396 references, there are cases where observed organisms are significantly structurally diverged  
397 (e.g. *Dialister*) and in one case bears minimal similarity to the available reference  
398 (*Subdoligranulum*).

399

### 400 Supplementary Figure 4

401 Homopolymer count as a function of length, and homopolymer error in assembled  
402 sequence as a function of length in corrected sequence. We found that uncorrected long read

403 assembly demonstrated a 3% error rate with 3-mer homopolymers, assembled too short by an  
404 average of 0.5 nucleotides. This worsens to a 65% error rate on 6-mer homopolymers, which  
405 were assembled too short by an average of 1.3 nucleotides. On average, 63 homopolymers of  
406 length 3 or greater were found per kilobase of assembled sequence, of which 4.5 (7.1%) were  
407 found to require correction with short reads.

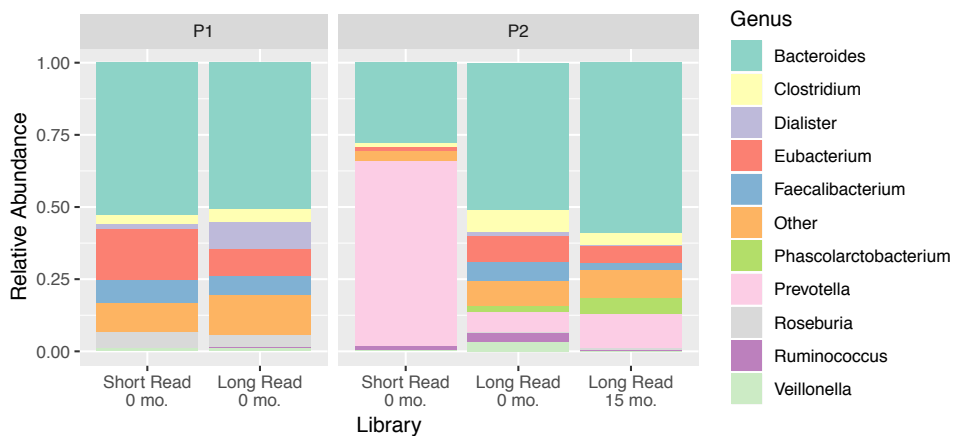
408

409 Supplementary Figure 5

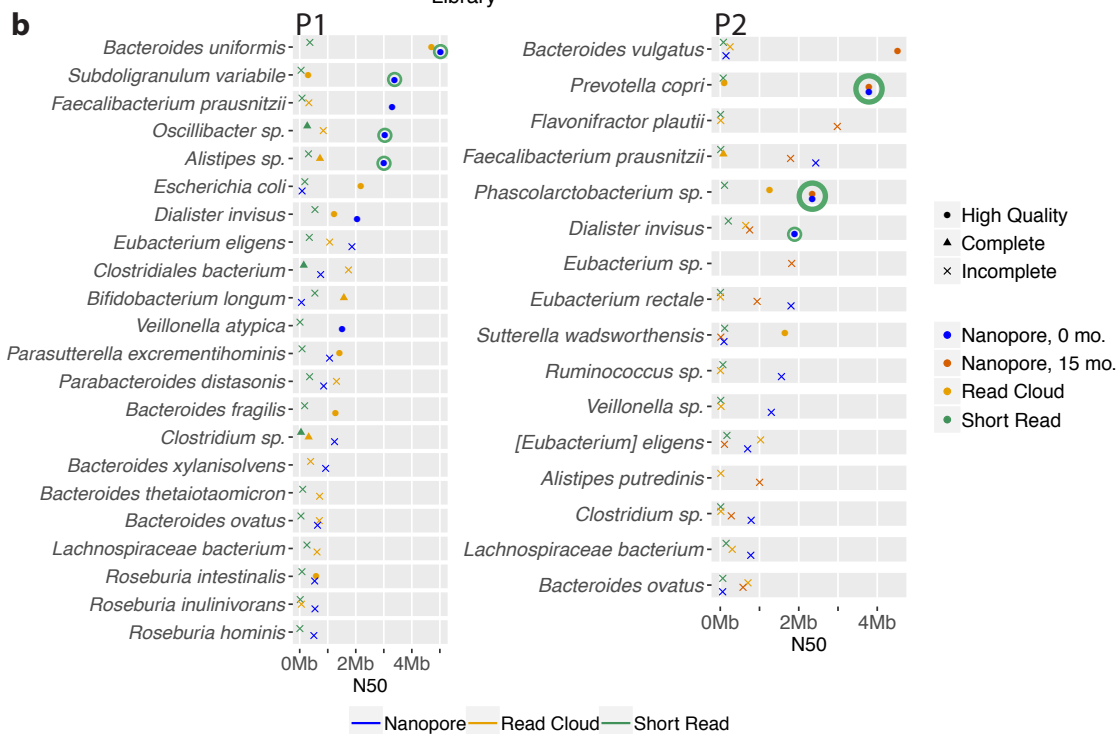
410 Nanopore long read assembly in some cases produces over-circularized genomes.  
411 These are sequences that are assembled beyond the wrap-around point, resulting in (a)  
412 redundant sequence which are detected and trimmed with the Encircle utility (present study).  
413 These sequences can be visualized as (b) corner-cutting off-diagonal alignments within contig  
414 self-alignment dotplots, such as that shown for the untrimmed *Subdoligranulum variabile*  
415 assembly.

# Figure 1

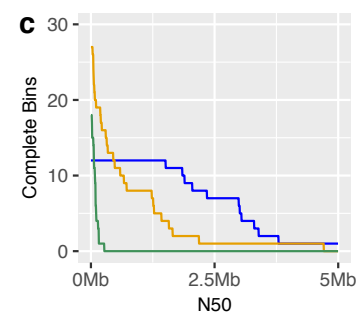
**a**



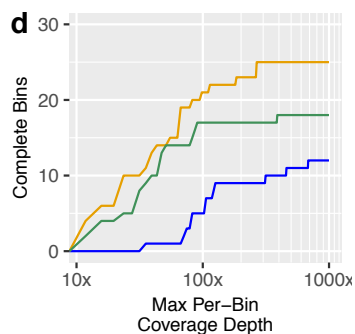
**b**



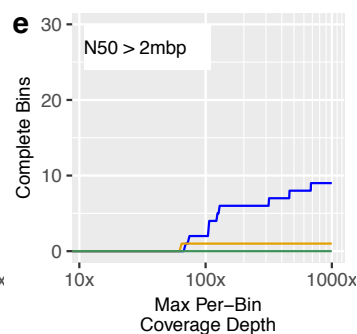
**c**



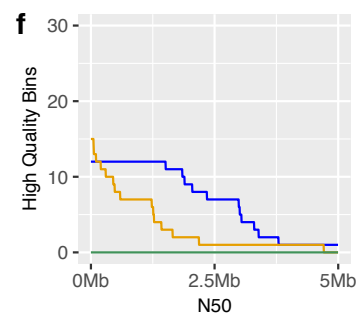
**d**



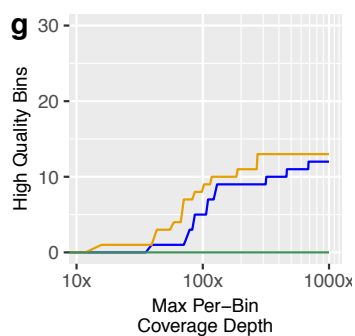
**e**



**f**



**g**



**h**

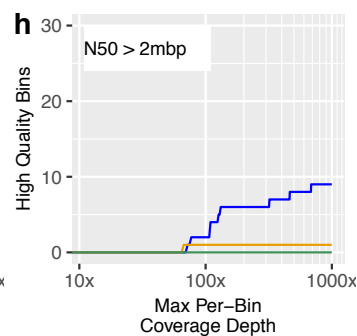
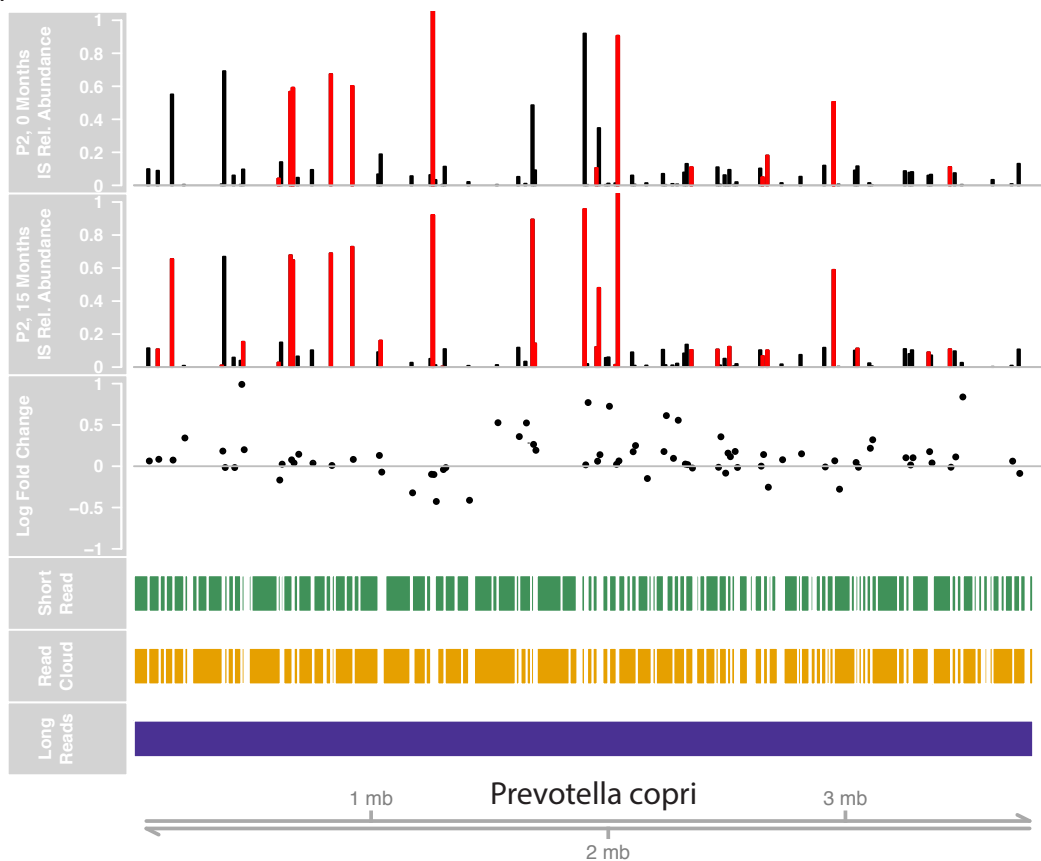


# Figure 2

a



b

